

Grazing-incidence X-ray fluorescence analysis for non-destructive determination of In and Ga depth profiles in Cu(In,Ga)Se₂ absorber films

C. Streeck,^{1,2} S. Brunken,¹ M. Gerlach,² C. Herzog,³ P. Hönicke,² C.A. Kaufmann,¹ J. Lubeck,² B. Pollakowski,² R. Unterumsberger,² A. Weber,¹ B. Beckhoff,² B. Kanngießner,³ H.-W. Schock,¹ and R. Mainz^{1,a)}

¹ Helmholtz-Zentrum Berlin für Materialien und Energie, Hahn-Meitner-Platz 1, 14109 Berlin, Germany

² Physikalisch-Technische Bundesanstalt, Abbestr.2-12, 10587 Berlin, Germany

³ Institute für Optik und Atomare Physik, Technische Universität Berlin, Hardenbergstr. 36, 10623 Berlin, Germany

Development of highly efficient thin film solar cells involves band gap engineering by tuning their elemental composition with depth. Here we show that grazing incidence X-ray fluorescence (GIXRF) analysis using monochromatic synchrotron radiation and well-characterized instrumentation is suitable for a non-destructive and reference-free analysis of compositional depth profiles in thin films. Variation of the incidence angle provides quantitative access to the in-depth distribution of the elements, which are retrieved from measured fluorescence intensities by modeling parameterized gradients and fitting calculated to measured fluorescence intensities. Our results show that double Ga gradients in Cu(In_{1-x}Ga_x)Se₂ can be resolved by GIXRF. © 2013 AIP Publishing LLC. [<http://dx.doi.org/10.1063/1.4821267>]

The physical properties of compound semiconductors depend on their elemental composition and hence, on the spatial distribution of their elements. The band gap of the compound semiconductor material Cu(In_{1-x}Ga_x)Se₂ can be enhanced by increasing the Ga to In ratio. Similarly, the band gap of many other alloys of compound semiconductors can be tuned by means of their elemental compositions. In thin film solar cells, the in-depth tunability of the band gap of the absorber film is utilized to increase open circuit voltage and to reduce back contact recombination.^{1,2} Therefore, a detailed understanding and optimization of the solar cell performance requires a precise and reliable determination of the elemental depth distributions. For this task, non-destructive depth profiling methods are particularly attractive as they are in principle suitable for in-line process control and for real-time investigations during film deposition or reactive annealing processes.³

The problem of an unambiguous and quantitative determination of elemental depth profiles in thin films such as Cu(In_{1-x}Ga_x)Se₂ is not yet solved, as shown by Abou-Ras et al. in a comprehensive assessment of various depth-profiling methods.⁴ While standard methods such as secondary ion mass spectrometry (SIMS) or cross-sectional energy-dispersive X-ray spectrometry analysis (EDX) show a satisfactory agreement of the qualitative depth profiles, quantitative analyses rely on well-defined reference material, a reliable control of the probing volume and on additional determination of the overall composition, e.g. by X-Ray fluorescence analysis (XRF). Moreover, common standard depth-profiling techniques are destructive. For a non-destructive determination of depth distributions in thin films, Kötschau et al. utilized grazing-incidence X-ray diffraction (GIXRD).^{5,4} However, with GIXRD only purely crystalline samples can be fully characterized, phase properties have to be well known, and the results may be distorted by mechanical strain, texture or grain size effects.

^{a)} Author to whom correspondence should be addressed. Electronic mail: roland.mainz@helmholtz-berlin.de

To overcome this problem, we employ grazing incidence X-Ray fluorescence analysis (GIXRF) for a quantitative analysis of the elemental depth distributions. GIXRF is not affected by the crystallographic properties of the characterized material and hence, in principle no foreknowledge of the properties of the samples is necessary.

Previously, we have analyzed the principle capability of synchrotron-based GIXRF to discriminate variations in Ga distributions in $\text{Cu}(\text{In}_{1-x}\text{Ga}_x)\text{Se}_2$.⁶ This discrimination capability is a necessary prerequisite for the principle ability to extract Ga distributions from measured GIXRF data.

Here, we now show that Ga depth profiles in $\text{Cu}(\text{In}_{1-x}\text{Ga}_x)\text{Se}_2$ thin films can be quantitatively determined with GIXRF by modeling depth distributions and fitting calculated fluorescence intensities to measured data. Well-defined monochromatic synchrotron radiation and radiometrically calibrated instrumentation is employed for the GIXRF experiments. A schematic drawing of the GIXRF measurement scheme is shown in Fig 1. The incidence angle between sample surface and incidence radiation was varied to tune the penetration depth, thus varying correspondingly the information depth of the fluorescence signals. Therefore, the fluorescence intensities measured under different incidence angles contain different information about the depth distributions of the elements. However the depth distributions cannot be directly derived from the angular dependent fluorescence intensities since for all incidence angles the measured intensities contain integral information originating from the entire excited probing volume in the film. A change of the incidence angle merely changes the weighting of the contributions from different depths. The main challenge of the method therefore is the reconstruction of the depth distributions from the complete set of the measured angular dependent fluorescence intensities.

To reconstruct depth profiles from the measured fluorescence intensities, a three-stage algorithm based on a *least square* adjustment procedure is applied to match calculated intensities to measured intensities by modeling parameterized depth distributions. This approach necessitates a high accuracy of both the measurement and the calculation. The latter relies on the precision of the employed fundamental X-ray atomic parameters as well as on the appropriate consideration of secondary effects contributing to the fluorescence intensities.

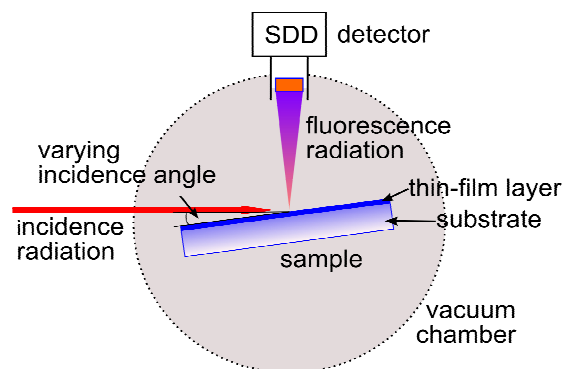


FIG. 1: Schematic drawing of the angular dependent grazing-incidence X-ray fluorescence measurements as a top view. The incidence angle between the incidence radiation of 11 keV and the sample is varied from 0° up to 25° . The angle between the silicon drift detector (SDD) and the incidence radiation is fixed at 90° . The investigated $\text{Cu}(\text{In}_{1-x}\text{Ga}_x)\text{Se}_2$ layers were a few μm thick and the glass substrate 2 mm thick.

To investigate the elemental depth profiling capability of GIXRF, $\text{Cu}(\text{In}_{1-x}\text{Ga}_x)\text{Se}_2$ thin films were synthesized with different Ga depth profiles by means of the standard three-stage co-evaporation process. Details on the process can be found in Refs. 7 and 8. A variation of the Ga depth distribution was achieved by the use of two different maximum temperatures of 530°C and 430°C during film synthesis.⁸ Both samples were prepared on molybdenum-

coated soda-lime glass substrates. The adopted processing temperatures are of particular interest for solar cell fabrication since the first one is the highest temperature that can be imposed on standard soda-lime glass without causing deformation of the substrate due to softening; the latter is low enough to be able to use polyimide foils as flexible substrate.⁸

GIXRF measurements were performed at the four-crystal monochromator (FCM) beamline⁹ in the laboratory of Physikalisch-Technische Bundesanstalt (PTB) at the electron storage ring BESSY II. At this bending magnet beamline, monochromatic synchrotron radiation of high spectral purity is available. A photon energy of 11 keV was used in order to excite the Cu K, Ga K and In L fluorescence. The beam profile has a size of approximately 300 μm x 200 μm . Measurements were performed in an ultra-high vacuum chamber equipped with a 9-axis manipulator.¹⁰ For the detection of fluorescence radiation an energy-dispersive silicon drift detector (SDD) was placed perpendicular to the incident beam within the orbital plane to reduce scattered excitation radiation to a minimum. The detector was calibrated and characterized by PTB, so that its response functions and detection efficiency are well known.¹¹ The incidence photon flux was determined by a calibrated photo diode. To determine the net fluorescence count rates, measured spectra for each angle of incidence were deconvoluted and fitted, taking into account the detector response functions¹² as well as modeled background contributions from Bremsstrahlung and resonant Raman scattering.¹³ To deconvolute the spectral contributions of the three In-L subshells, constant multiplets of the fluorescence lines associated with each subshell were employed, which were derived from additional measurements on an In foil.¹⁴ The count rates obtained from the deconvolution were then converted to fluorescence intensities by using the efficiency of the SDD, and by normalization to both the incident photon flux and the effective solid angle of detection.

The normalized fluorescence intensities of the Ga K α , In L α and Cu K α lines are shown in Fig. 2 as function of the incidence angle for the Cu(In_{1-x}Ga_x)Se₂ samples synthesized at 430 °C and 530 °C. The differences of the fluorescence intensities between the two different samples are larger than the total error limits of the measurements (see Fig. S3 in Supplemental Material¹⁵), indicating that the two samples have different depth distributions distinguishable by GIXRF. According to Lambert-Beer's law, the contribution of a region of the sample to a fluorescence signal decreases with increasing depth, whereas an increase of the incidence angle leads to an increase of the contribution from deeper regions. Consequently, at shallow incidence angles the fluorescence intensities of the surface-near region dominate whereas with increase of the incidence angle the contributions of deeper parts of the layer to the fluorescence signals increase. It can be seen that for the 430 °C sample, the Ga fluorescence intensity between 1.5° and 4° decreases much faster than those for the 530 °C sample (in Fig. 2a). This indicates that the 430 °C sample features a stronger decrease of the Ga concentration with increasing depth. The In fluorescence signals show only small difference between the two samples (Fig. 2b). Due to a relatively short attenuation length for the In L α fluorescence radiation, even at large angles the In L α intensity is dominated by the front part of the sample (see Supplementary Material for details¹⁶). Thus, the similarity of the signals indicates that in the front part the two samples feature similar In concentrations. Additionally, in the investigated samples the In concentration is higher than that of Ga (see Supplemental Material¹⁷) and thus the relative variation of the In concentration can be expected to be smaller compared to that of Ga, leading to a smaller angular dependence of the In fluorescence on the In depth distribution. The Cu fluorescence signals show a large difference which becomes smaller with increasing incidence angle (Fig. 2c). This behavior can be explained by a depleted Cu concentration at the surface of the 430 °C film. At higher incidence angles, the fluorescence intensity curves for all fluorescence lines converge to similar values. This indicates approximately equal integral mass deposition of the two samples.

For a quantitative reconstruction of the elemental depth profiles from the GIXRF data shown in Fig. 2, modeling of the angular dependency of the respective fluorescence lines is necessary. Our approach involves forward calculations of the fluorescence intensities assuming a parameterized model elemental depth profile. The resulting calculated angular dependent intensities are then compared with the measured angular dependent intensities. From the difference between calculated and measured intensities, a total error square χ^2 is determined. A least square method using the Levenberg-Marquardt algorithm is then employed to find the depth profile that leads to a best fit between the GIXRF measurements and the calculations.

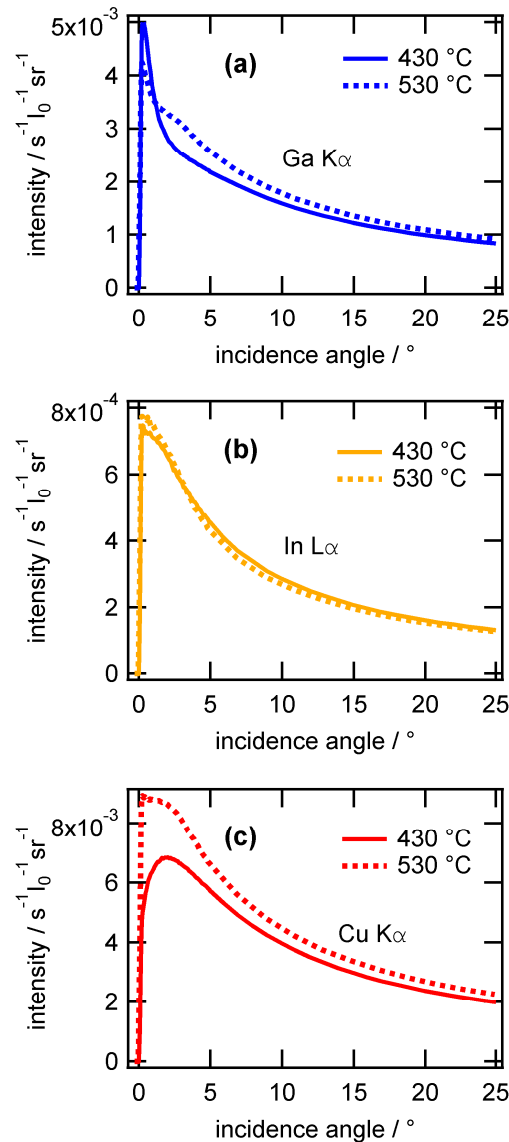


FIG. 2: Grazing-incidence X-ray fluorescence intensities for (a) Ga K α , (b) In L α and (c) Cu K α in dependence of the angle of incidence for two different Cu(In,Ga)Se₂ films synthesized by three-stage co-evaporation process at 430 °C and 530 °C.

To obtain a stable fit, a simple model gradient was chosen in this study, which approximates the Ga/In depth gradient to be double-linear and the Cu concentration to be constant over the depth. According to this model, the Ga concentration is allowed to have a minimum or maximum between the surface and the bottom of the film. The model gradient is described by six parameters: the [Ga]/([Ga]+[In]) ratio (1) at the front, (2) at a point between front and back, (3) and at the back of the thin film, (4) the position of the point between front

and back, (5) the overall $[Cu]/([Ga]+[In])$ ratio and (6) the thickness of the film. The Se concentration is calculated from the Ga, In and Cu concentration with the assumption that the composition of the film follows the pseudo-binary $Cu_2Se-(In,Ga)_2Se_3$ phase diagram.¹⁸

For the calculation of the angular dependent fluorescence intensities, the film is subdivided into 25 sublayers. The concentrations within each sublayer are assumed to be homogeneous as a convenient approximation. The individual thicknesses of the respective sublayers are chosen to increase with increasing depth to account for the decreasing sensitivity of the method with increasing distance from the film surface. The calculation takes into account primary and secondary fluorescence effects. (For an investigation of the contribution by secondary fluorescence to the total fluorescence for $Cu(In,Ga)Se_2$ films, see Ref. 3). Relevant atomic fundamental X-ray parameters such as the fluorescence yield, the photo ionization cross sections and the total absorption cross-sections are employed. The effective fluorescence production cross section, including the Coster-Kronig transitions for In $L\alpha$ at 11 keV has been newly determined according to Ref. 14.

The modeling routine for the determination of the depth distributions from the GIXRF data consists of the following steps: (i) The measurement at the maximum angle of incidence is used to determine an integral Cu concentration (parameter 5) and the overall thickness (6) under assumption of a homogeneous $Cu(In_{1-x}Ga_x)Se_2$ layer. (ii) To obtain an initial guess for parameter 1, the fluorescence intensities at incidence angles up to 0.2° are employed to determine the $[Ga]/([Ga]+[In])$ ratio at the front of the layer. (iii) All parameters except parameter 5 are refined by the least square fit to find the best match between calculated and measured fluorescence intensities.

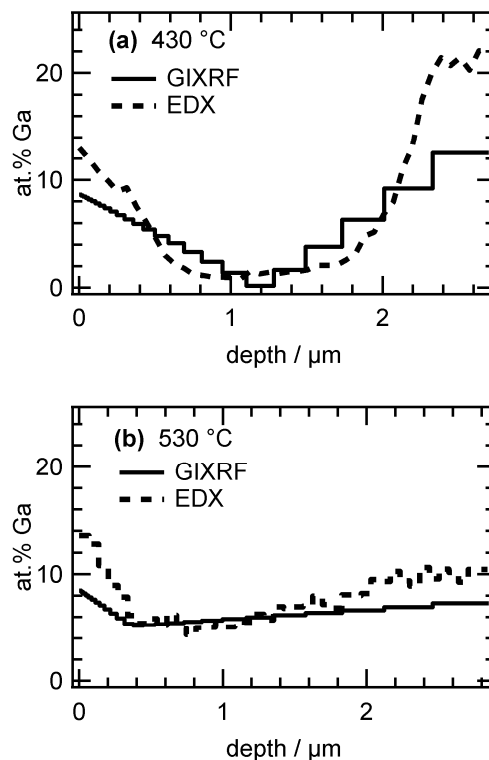


FIG. 3: Ga depth distributions resulting from the fit of grazing-incidence X-ray fluorescence (GIXRF) data and from cross-sectional energy-dispersive X-ray spectrometry (EDX) measurements for two different $Cu(In_{1-x}Ga_x)Se_2$ sample synthesized by a three-stage co-evaporation process at (a) $430^\circ C$ and (b) $530^\circ C$.

The Ga depth distributions retrieved from the GIXRF data by this procedure are plotted as solid lines in Figs. 3 for both samples, synthesized at 430 °C (a) and 530 °C (b). The step-like course of the lines reflects the subdivision of the film into sublayers. (The corresponding depth distributions for Cu and In can be found in Supplemental Material, Fig. S1.¹⁹) For both samples, the graphs show a double gradient nature of the Ga distributions with a minimum between the surface and the bottom of the films. The uncertainty of the position of the minimum resulting from the fit is $\pm 0.2 \mu\text{m}$. The result for the sample synthesized at 430 °C shows a more pronounced decrease of the Ga distribution in the center part of the film compared to the sample synthesized at 530 °C. This result is in agreement with the findings of Kaufmann *et al.*⁸ Such a Ga depth profile is detrimental for the solar cell performance since the steep Ga increase – implying a band gap increase – towards the front of the film, imposes a barrier for electrons between the p-type absorber and the n-type window layer²⁰. In contrast, the sample synthesized at 530 °C shows a typical shallow profile of the Ga distribution,⁴ leading to high solar cell conversion efficiencies.²⁰

The depth distributions resulting from the GIXRF data are compared with depth distributions determined by cross-sectional EDX measurements (dashed lines in Figs. 3) performed in a scanning electron microscope. The depth-dependent EDX intensities were scaled such that the integral compositions match the ones determined by means of a standard-based XRF instrumentation (see Supplemental Material for more details¹⁷). For both samples the positions of the minima of the modeled distributions are well in line with those of the distributions deduced from the EDX measurements. Also the compositions at the minimum of both methods show a close match. In contrast, the maximum Ga concentrations at the front and the back side of both films show much stronger deviations, with higher concentrations observed by EDX. It is difficult to judge which of the methods is closer to the true maximum compositions of the samples, since the precise error limits of both methods are not yet fully known. Apart from this it is clear that for a precise GIXRF analysis of depth profiles that deviate from a double linear shape, an extended depth distribution model with a larger number of free parameters is needed. In fact, for the best fit with the applied double linear model, the deviation of the calculated and measured fluorescence intensities is larger than the error limit of the GIXRF measurements (see Supplemental Material, Figs. S2 and S3¹⁵). This finding indicates that the true depth profile deviates from the double linear model, as was also observed by EDX (Fig. 3). An increase of free parameters leads to a decrease of the stability of the deployed Levenberg-Marquardt fit algorithm. Alternative, more robust fitting strategies shall be investigated in the future. In addition, fluorescence line intensities of additional shells of the elements and variation of the incidence radiation energy may have to be included in the measurement and adjustment procedure to further increase the information content, and thus to be able to increase the number of parameters that describe the depth profiles.

An increase of the number of parameters can reduce or eliminate the necessity of any foreknowledge of the elements and phases present in the sample. Thus, if accuracy of the measurements and the numerical calculation are further increased, quantitative characterization of samples with completely unknown composition and element distributions may become possible with this method.

In the presented study, we employed synchrotron radiation at a beam-line with calibrated instrumentation. The low divergence and well-known intensities of this radiation are ideal for the investigation of the capability of GIXRF, but makes it unsuitable for standard measurements or in-line process control. As X-ray sources,^{21,22} multilayer optics²³ and detector technologies^{24,25,26} develop rapidly, high X-ray fluorescence count rates on a lab-scale setup for in-line or other lab-size applications of this method should become feasible.

Besides these perspectives, the more elaborate synchrotron-based approach is attractive as reference measurement method, since GIXRF in combination with calibrated instrumentation provides quantitative access to the in-depth distribution of the elements. It hence can be

employed for the qualification and characterization of reference material, which then can be used for the calibration of other lab-scale depth-profiling methods. In particular, this is of interest for the investigation of new materials, when reference materials do not exist.

Moreover, with synchrotron radiation and presently available detector technology, already now real-time investigations of the evolution of quantitative Ga depth distributions during the growth of Cu(In,Ga)Se₂ films with a time resolution in the order of minutes are feasible, if fluorescence intensities under various exit angles are measured simultaneously.

In summary we conclude that GIXRF is suitable for reference free and non-destructive determination of elemental depth distributions in thin films. We have shown that Ga-In depth distributions in Cu(In_{1-x}Ga_x)Se₂ thin films with a double gradient can be reconstructed from angular dependent GIXRF measurements by modeling depth distributions and fitting calculated fluorescence intensities to the measured data. The depth distributions gained by this method are in good agreement with depth distributions measured by cross-sectional EDX.

The authors thank Sonja Cinque und Christian Wolf from PVcomB (Competence Centre Thin-Film- and Nanotechnology for Photovoltaics Berlin) for providing the standard XRF measurements. Fruitful discussions with Wolfgang Malzer and his contributions to the numerical calculations are highly acknowledged. This work was funded through the European Metrology Research Program (EMRP) Project IND07 Thin Films. The EMRP is jointly funded by the EMRP participating countries within EURAMET and the European Union.

Bibliography

- ¹ A. M. Gabor, J. R. Tuttle, M. H. Bode, A. Franz, A. L. Tennant, M. A. Contreras, R. Noufi, D. G. Jensen, and A. M. Hermann, *Sol. Energy Mater. Sol. Cells* **41/42**, 247 (1996).
- ² T. Dullweber, O. Lundberg, J. Malmström, M. Bodegard, L. Stolt, U. Rau, H. W. Schock, and J. H. Werner, *Thin Solid Films* **387**, 11 (2001).
- ³ R. Mainz and R. Klenk, *J. Appl. Phys.* **109**, 123515 (2011).
- ⁴ D. Abou-Ras, R. Caballero, C.-H. Fischer, C. Kaufmann, I. Lauermann, R. Mainz, H. Mönig, A. Schöpke, C. Stephan, S. Schorr, A. Eicke, M. Döbeli, B. Gade, J. Hinrichs, T. Nunney, H. Dijkstra, V. Hoffmann, D. Klemm, V. Efimova, A. Bergmaier, G. Dollinger, T. Wirth, W. Unger, A. Rockett, A. P. Rodriguez, J. A. Garcia, V. Izquierdo, T. Schmid, S. Zaefferer, A. Dempewolf, F. Bertram, J. Christen, M. Sestak, and R. Collins, *Microsc. Microanal.* **17**, 728 (2011).
- ⁵ I. M. Kötschau and H. W. Schock, *J. Appl. Crystallogr.* **39**, 683 (2006).
- ⁶ C. Streeck, B. Beckhoff, F. Reinhardt, M. Kolbe, B. Kanngießner, C.A. Kaufmann, H.W. Schock, *Nucl. Instrum. Meth. B*, **268** 277 (2010).
- ⁷ R. Caballero, C. Kaufmann, V. Efimova, T. Rissom, V. Hoffmann, and H. Schock, *Prog. Photovolt: Res. Appl.* **21**, 30 (2013).
- ⁸ C. Kaufmann, R. Caballero, T. Unold, R. Hesse, R. Klenk, S. Schorr, M. Nichterwitz, and H.-W. Schock, *Sol. Energ. Mat. Sol. Cells* **93**, 859–863 (2009).
- ⁹ M. Krumrey, M. Gerlach, F. Scholze, and G. Ulm, *Nucl. Instrum. Meth. A* **568** 364 (2006).
- ¹⁰ J. Lubeck, B. Beckhoff, R. Fliegau, I. Holfelder, P. Hönicke, M. Müller, B. Pollakowski, F. Reinhardt, and J. Weser, *Rev. Sci. Instrum.* **84**, 045106 (2013).
- ¹¹ M. Krumrey and G. Ulm, *Nucl. Instrum. Meth. A* **467-468** 1175 (2001).
- ¹² F. Scholze and M. Procop, *X-ray Spectrom.* **38**, 312 (2009).
- ¹³ M. Müller, B. Beckhoff, G. Ulm, and B. Kanngießner, *Phys. Rev. A* **74**, 012702 (2006).
- ¹⁴ M. Kolbe, P. Hönicke, M. Müller, and B. Beckhoff, *Phys. Rev. A* **86**, 042512 (2012).
- ¹⁵ See supplementary material at [URL will be inserted by AIP] for a comparison of the measured and calculated fluorescence intensities with the total error limits of the measurements.
- ¹⁶ See supplementary material at [URL will be inserted by AIP], for the information depth of GIXRF for a Cu(In,Ga)Se₂ film at incidence angles of 0.5° and 25°.
- ¹⁷ See supplementary material at [URL will be inserted by AIP] for details on the compositions of the Cu(In,Ga)Se₂ films.

-
- ¹⁸ R. Scheer and H.-W. Schock. *Chalcogenide Photovoltaics: Physics, Technologies, and Thin Film Devices*. (Wiley-VCH Verlag GmbH & Co. KGaA, Weinheim, 2011).
- ¹⁹ See supplementary material at [URL will be inserted by AIP] for depth distributions of Ga, In and Cu determined by GIXRF and by EDX.
- ²⁰ A. Chirila, S. Buecheler, F. Pianezzi, P. Bloesch, C. Gretener, A. R. Uhl, C. Fella, L. Kranz, J. Perrenoud, S. Seyrling, R. Verma, S. Nishiwaki, Y. E. Romanyuk, G. Bilger and A. N. Tiwari, *Nat. Mater.* **10**, 857 (2011).
- ²¹ O. Hemberg, M. Otendal, and H. M. Hertz, *Appl. Phys. Lett.*, **83**, 1483 (2003).
- ²² I. Mantouvalou, R. Jung, J. Tuemmler, H. Legall, T. Bidu, H. Stiel, W. Malzer, B. Kanngießer, and W. Sandner, *Rev. Sci. Instrum.* **82**, 066103 (2011).
- ²³ R. Dietsch, T. Holz, M. Krämer, und D. Weißbach, *Proc. SPIE 7995*, Seventh International Conference on Thin Film Physics and Applications, 79951U, Shanghai, China, September 24 2010, edited by J. Chu and Z. Wang (February 17, 2011 2011), doi:10.1117/12.888192.
- ²⁴ L. Strüder, S. Epp, D. Rolles, R. Hartmann, P. Holl, G. Lutz, H. Soltau, R. Eckart, C. Reich, K. Heinzinger, C. Thamm, A. Rudenko, F. Krasniqi, K.-U. Kühnel, C. Bauer, C.-D. Schröter, R. Moshhammer, S. Techert, D. Miessner, M. Porro, O. Hälker, N. Meidinger, N. Kimmel, R. Andritschke, F. Schopper, G. Weidenspointner, A. Ziegler, D. Pietschner, S. Herrmann, U. Pietsch, A. Walenta, W. Leitenberger, C. Bostedt, T. Möller, D. Rupp, M. Adolph, H. Graafsma, H. Hirsemann, K. Gärtner, R. Richter, L. Foucar, R. L. Shoeman, I. Schlichting, and J. Ullrich, *Nucl. Instrum. Meth. A*, **614**, 483 (2010).
- ²⁵ M. Porro, D. Bianchi, G. De Vita, R. Hartmann, G. Hauser, S. Herrmann, L. Struder, and A. Wassatsch, *IEEE T. Nucl. Sci.*, **60**, 446 (2013).
- ²⁶ J. C. Woicik, B. Ravel, D. A. Fischer and W. J. Newburgh, *J. Synchrotron Radiat.* **17**, 409 (2010).